Quantum Chemical Investigation and Experimental Verification on the Aquatic Photochemistry of the Sunscreen 2-Phenylbenzimidazole-5-Sulfonic Acid

ARTICLE *in* ENVIRONMENTAL SCIENCE & TECHNOLOGY · OCTOBER 2010

Impact Factor: 5.33 · DOI: 10.1021/es101131h · Source: PubMed

6 AUTHORS, INCLUDING:

Siyu Zhang
Institute of Applied Ecology, Chinese Acad…
13 PUBLICATIONS **208** CITATIONS
SEE PROFILE

Xianliang Qiao
Dalian University of Technology
55 PUBLICATIONS **1,119** CITATIONS
SEE PROFILE

Xiyun Cai
Dalian University of Technology
40 PUBLICATIONS **761** CITATIONS
SEE PROFILE

Guangshui Na
National Marine Environmental Monitoring…
43 PUBLICATIONS **291** CITATIONS
SEE PROFILE

Environ. Sci. Technol. **2010,** *44,* 7484–7490

Quantum Chemical Investigation and Experimental Verification on the Aquatic Photochemistry of the Sunscreen 2-Phenylbenzimidazole-5-Sulfonic Acid

SIYU ZHANG,[†] JINGWEN CHEN,*[,†] XIANLIANG QIAO,[†] LINKE GE,[‡] XIYUN CAI,[†] AND GUANGSHUI NA[‡]

Key Laboratory of Industrial Ecology and Environmental Engineering (MOE), School of Environmental Science and Technology, Dalian University of Technology, Dalian 116024, P. R. China, and National Marine Environmental Monitoring Center, Dalian 116023, P. R. China

Received April 9, 2010. Revised manuscript received August 27, 2010. Accepted August 29, 2010.

For ecological risk assessment of the large and ever-increasing number of chemical pollutants, it is of importance to develop computational methods to screen or predict their environmental photodegradation behavior. This study developed a computational method based on the density functional theory (DFT) to predict and evaluate the photodegradation behavior and effects of water constituents, taking a sunscreen and personal care product 2-phenylbenzimidazole-5-sulfonic acid (PBSA) as a model compound. Energy and electron transfer reactions of excited state PBSA (PBSA*) with $^3O_2$ and water constituents were evaluated. The computational results indicated that PBSA* could photogenerate $^1O_2$ and $O_2^{-}\cdot$, triplet excited state humic/fulvic acid analogs could not photosensitize the degradation, and the anions (Cl^-, Br^-, and HCO_3^-) could not quench PBSA* or its radical cation chemically. Experiments employing simulated sunlight confirmed that PBSA photodegraded via the direct and self-sensitization mechanism involving $O_2^{-}\cdot$. The photodegradation was pH-dependent. The direct and self-sensitized photodegradation was inhibited by fulvic acid. The main photodegradation products were identified, and the pathways were clarified. These results indicate that the DFT-based computational method can be employed to assess the environmental photochemical fate of organic pollutants.

Introduction

Sunscreens are widely used in personal care products (*1*), polymers, and pigments (*2*). Due to the growing awareness of the need of prevention from skin cancer, the consumption of sunscreens is increasing. Recently, these compounds have been found ubiquitously in natural water, drinking water, and wastewater (*3*−*5*). Some of them have estrogenic activity (*6, 7*) and are phytotoxic (*8*), and their toxicity may be altered by solar irradiation (*8, 9*). Moreover, some sunscreens can photogenerate reactive oxygen species (ROS) (*10*−*12*) that may damage biomacromolecules. For example, 2-phenylbenzimidazole-5-sulfonic acid (PBSA), a widely used sunscreen, can photogenerate $^1O_2$ and $O_2^{-}\cdot$ (*12*) and cause DNA damage (*13*). Thus, it deserves special attention to understand the photochemical behavior and fate of sunscreens for the purpose of ecological risk assessment.

Clarifying the photodegradation mechanisms is of great importance to understand the risk of aquatic pollutants (*14*−*19*). The photochemical fate of organic pollutants is influenced by water constituents, e.g., NO_3^-, NO_2^-, dissolved organic matter (DOM), halide ions (X^-), and HCO_3^-/CO_3^{2-} (*14*−*21*). Sakkas et al. (*22*) investigated the photodegradation of a sunscreen, octyl-dimethyl-*p*-aminobenzoic acid, in pure water, seawater, and swimming pool water, and found the photolysis rate was inhibited by humic acid (HA). Giokas et al. (*23*) found the photolysis kinetics of two sunscreens, 3-(4-methylbenzyldene)-camphor and octyl-methoxycinnamate, to be dependent on the multivariate effects of HA, Cl^-, and NO_3^-. Klein et al. (*24*) assessed the relative importance of direct and indirect photolysis for octyl-methoxycinnamate and homosalate in surface waters and proposed photodegradation pathways for octyl-methoxycinnnamate.

The photolysis of some sunscreens was proven to be O_2-dependent (*25*). Allen et al. (*10*) found that $^1O_2$ could be photogenerated by a sunscreen, *p*-aminobenzoic acid (PABA), and determined the second-order reaction rate constant of PABA with $^1O_2$ (*26*). Shaw et al. (*27*) suggested that O_2 was involved in the photodegradation of PABA. These observations imply that some sunscreens can undergo self-sensitized photooxidation, in addition to direct and indirect photodegradation. However, the ROS generating pathways and photodegradation products for many sunscreens have not yet been explored.

In addition to ROS, other radicals may also be involved in the photochemical reactions. Previous studies observed formation of halogenated radicals ($X\cdot/X_2^{-}\cdot$) (*28, 29*) and carbonate radicals ($CO_3^{-}\cdot$) (*30, 31*), generated from photosensitizing reactions of chlorophyll and aromatic ketones/sulfonates. $X\cdot/X_2^{-}\cdot$ can produce halogenated compounds (*32, 33*). Thus, special concern should be focused on the photogeneration and effects of these radicals.

Given the huge and ever-increasing number of emerging organic pollutants (*1*), it is important to develop computational screening methods to evaluate the photochemical reaction pathways, as experimental methods are costly and time-consuming, and cannot evaluate all emerging chemicals. In this study, a computational method was developed based on the density functional theory (DFT) to investigate the photodegradation behavior of PBSA. PBSA was selected as a model compound, since it was observed to photogenerate $^1O_2$ and $O_2^{-}\cdot$, and to accept electron transfer from N_3^- (*12*). However, the ROS generating pathways, photodegradation mechanism, and effects of water constituents on PBSA photodegradation were still unclear.

The electron or energy transfer reactions between electronically excited state PBSA* and ground state oxygen ($^3O_2$) or water constituents were evaluated. DFT was adopted as it has been successfully applied to predict the energy and electron transfer from excited state molecules to $^3O_2$ (*34, 35*). The results predicted by DFT were experimentally verified. The photodegradation products were analyzed, and the photodegradation mechanism was clarified. This study not only contributes to ecological risk assessment of the sunscreen, but also presents a potential method for evaluating the photodegradation mechanisms

* Corresponding author phone/fax: +86-411-84706269; e-mail: jwchen@dlut.edu.cn.
[†] Dalian University of Technology.
[‡] National Marine Environmental Monitoring Center.

10.1021/es101131h

Published on Web 09/13/2010

TABLE 1. Photoinduced Energy and Electron Transfer Reactions between PBSA and $^3O_2$ or Water Constituents and Corresponding Evaluating Criteria

no.	reaction	criterion
1	$PBSA^*_{sl} + {}^3O_2({}^3\Sigma_g^-) \rightarrow PBSA^*_{Tl} + {}^1O_2({}^1\Sigma_g^+)$	$E_{S1} - E_{T1} > E_\Sigma$[a]
2	$PBSA^*_{S1} + {}^3O_2({}^3\Sigma_g^-) \rightarrow PBSA^*_{T1} + {}^1O_2({}^1\Delta_g)$	$E_{S1} - E_{T1} > E_\Delta$[b]
3	$PBSA^*_{T1} + {}^3O_2({}^3\Sigma_g^-) \rightarrow PBSA_{S0} + {}^1O_2({}^1\Sigma_g^+)$	$E_{T1} > E_\Sigma$
4	$PBSA^*_{T1} + {}^3O_2({}^3\Sigma_g^-) \rightarrow PBSA_{S0} + {}^1O_2({}^1\Delta_g)$	$E_{T1} > E_\Delta$
5	$PBSA^*_{S1/T1} + {}^3O_2 \rightarrow PBSA^+\cdot + O_2^-\cdot$	$\Delta G_1 = AEA({}^3O_2) + VIE_{S1/T1} < 0$
6	$PBSA^*_{S1/T1} + PBSA_{S0} \rightarrow PBSA^+\cdot + PBSA^-\cdot$	$\Delta G_2 = VEA_{S0} + VIE_{S1/T1} < 0$ $\Delta G_3 = VEA_{S1/T1} + VIE_{S0} < 0$[c]
7	$PBSA^*_{S1/T1} + PBSA^*_{S1/T1} \rightarrow PBSA^+\cdot + PBSA^-\cdot$	$\Delta G_4 = VEA_{S1/T1} + VIE_{S1/T1} < 0$
8	$PBSA^-\cdot + {}^3O_2 \rightarrow PBSA_{S0} + O_2^-\cdot$	$\Delta G_5 = AEA({}^3O_2) + VIE_{S0}(PBSA^-\cdot) < 0$[d]
9	$ADOM^*_{T1} + PBSA_{S0} \rightarrow PBSA^*_{T1} + ADOM_{S0}$	$E_{T1}(ADOM) > E_{T1}(PBSA)$
10	$ADOM^*_{T1} + PBSA_{S0} \rightarrow ADOM^-\cdot + PBSA^+\cdot$	$\Delta G_6 = VEA_{T1}(ADOM) + VIE_{S0} < 0$
11	$ADOM^*_{T1} + PBSA_{S0} \rightarrow ADOM^+\cdot + PBSA^-\cdot$	$\Delta G_7 = VIE_{T1}(ADOM) + VEA_{S0} < 0$
12	$PBSA^*_{S1} + D^- \rightarrow PBSA^-\cdot + D\cdot$[e]	$\Delta G_8 = VEA_{S1} + VIE(D^-) < 0$
13	$PBSA^*_{T1} + D^- \rightarrow PBSA^-\cdot + D\cdot$	$\Delta G_9 = VEA_{T1} + VIE(D^-) < 0$
14	$PBSA^+\cdot + D^- \rightarrow PBSA + D\cdot$	$\Delta G_{10} = VIE(D^-) + VEA_{S0}(PBSA^+\cdot) < 0$[f]

[a] E_{S1} and E_{T1} are the lowest singlet and triplet excitation energies of PBSA, respectively; E_Σ is the excitation energy of $^3O_2$ ($^3\Sigma_g^-$) to $^1O_2$ ($^1\Sigma_g^+$). [b] E_Δ is the excitation energy of $^3O_2$ ($^3\Sigma_g^-$) to $^1O_2$ ($^1\Delta_g$). [c] ΔG_2 and ΔG_3 are for the electron transfer reactions with $PBSA_{S0}$ as electron acceptor and donor, respectively. [d] $VIE_{S0}(PBSA^-\cdot) = -VEA_{S0}(PBSA)$. [e] D^- stands for N_3^-, X^-, HCO_3^-, and CO_3^{2-}. [f] $VEA_{S0}(PBSA^+\cdot) = -VIE_{S0}(PBSA)$.

of organic pollutants. It is worth mentioning that ·OH also plays an important role in the photodegradation (*14*, *16*, *18*, *20*), and the photodegradation of PBSA may involve ·OH. However, ·OH was beyond the scope of the current study as the essence of the question was to evaluate the reactivity with ·OH.

Materials and Methods

Chemicals. Sources of the chemicals used in the study are described in the Supporting Information (SI).

Computational Methods. The three pH-dependent protonation states of PBSA (Figure S1 in SI): neutral (PBSA0), monoanion (PBSA-H), and dianion (PBSA-2H), were considered in the computation. The ROS generating reactions are essentially processes of energy and electron transfer from the singlet/triplet excited PBSA ($PBSA^*_{S1/T1}$) to $^3O_2$($^3\Sigma_g^-$) (*36*, *37*). For the photogeneration of $^1O_2$($^1\Sigma_g^+$ and $^1\Delta_g$), four spin-allowed energy transfer reactions, from $PBSA_{S1}$ to $PBSA_{T1}$ and from $PBSA_{T1}$ to $PBSA_{S0}$, were considered (Reactions 1−4, Table 1). The possibilities of these reactions were evaluated

TABLE 2. Computed Values for the Excitation Energy, Vertical Ionization Energy, and Vertical Electron Affinity of PBSA, DOM Analogs, and Anions[a]

species	E_{S1}	E_{T1}	$E_{S1} - E_{T1}$	VIE_{S0}	VEA_{S0}	VIE_{S1}	VEA_{S1}	VIE_{T1}	VEA_{T1}
PBSA0	4.085	2.954	1.131	6.457	−2.220	2.372	−6.305	3.503	−5.174
PBSA-H	4.045	2.913	1.132	6.139	−1.946	2.094	−5.991	3.226	−4.859
PBSA-2H	3.837	2.951	0.886	5.267	−1.307	1.430	−5.144	2.316	−4.258

DOM analogs	E_{T1}	VIE_{S0}	VEA_{S0}	VIE_{T1}	VEA_{T1}
LHA	2.233	6.251	−3.768	4.018	−6.001
CSHA	2.597	6.295	−2.732	3.698	−5.329
ARHA	2.537	6.427	−2.624	3.890	−5.161
SRFA	2.371	5.732	−2.166	3.361	−4.537

anions	Cl^-	Br^-	I^-	HCO_3^-	CO_3^{2-}
VIE	6.715	6.359	5.671	6.589	4.282

[a] The unit of the energy is eV.

by the lowest singlet (E_{S1}) and triplet (E_{T1}) excitation energies of PBSA, and the excitation energy of $^3O_2(^3\Sigma_g^-)$ to $^1O_2(^1\Sigma_g^+)$ or $^1O_2(^1\Delta_g)$, which were expressed as E_Σ and E_Δ, respectively.

The excited state molecules can also photogenerate $O_2^{-}\cdot$ via electron transfer. The electron donating ability (EDA) and electron accepting ability (EAA) were evaluated by the vertical ionization energy (VIE) and vertical electron affinity (VEA), respectively. A low VIE value implies strong EDA, and a low VEA value implies strong EAA. The electron transfer reaction was determined by the overall change in the Gibbs free energy (ΔG); $\Delta G < 0$ means that the reaction is spontaneous (*37*). ΔG for bimolecular reactions was calculated by eq 1, where VIE and VEA for excited state molecules were computed by eqs 2 and 3, respectively.

$$\Delta G = \mathrm{VIE} + \mathrm{VEA} \quad (1)$$

$$\mathrm{VIE_{S1}} = \mathrm{VIE_{S0}} - E_{S1},\ \mathrm{VIE_{T1}} = \mathrm{VIE_{S0}} - E_{T1} \quad (2)$$

$$\mathrm{VEA_{S1}} = \mathrm{VEA_{S0}} - E_{S1},\ \mathrm{VEA_{T1}} = \mathrm{VEA_{S0}} - E_{T1} \quad (3)$$

The adiabatic electron affinity (AEA) was employed to evaluate the EAA of $^3O_2$ (*34, 35*). Two possible pathways were considered in the $O_2^{-}\cdot$ generation. The first pathway was the direct electron transfer from $PBSA^*_{S1/T1}$ to $^3O_2$ (Reaction 5, Table 1). The second pathway involved the PBSA radical anion ($PBSA^{-}\cdot$) formed through autoionization (Reactions 6 and 7, Table 1) and the electron transfer from $PBSA^{-}\cdot$ to $^3O_2$ (Reaction 8, Table 1).

Energy and electron transfer can also take place between PBSA* and water constituents, including DOM, X^-, and HCO_3^-/CO_3^{2-}, etc. (Reactions 9−14, Table 1). Some analog structures of DOM (ADOM) from different origins (Figure S2) were employed for the computation, including the Leonardite humic acid (LHA) (*38*), the Chelsea soil humic acid (CSHA) (*39*), the Altamaha River humic acid (ARHA) (*40*), and the Suwannee River fulvic acid (SRFA) (*41*). To validate the computational method for evaluating electron transfer between PBSA* and anions, N_3^- was included in the computations, since the experimental data for the reaction of N_3^- with PBSA were available (*12*). All the evaluated photosensitizing pathways are summarized in Figure S3.

All the DFT computations were performed using the Gaussian 09 software package (*42*) with the B3LYP functional (*43, 44*). The bulk solvent effect of water was considered by using the integral equation formalism polarized continuum model (IEFPCM) based on the self-consistent-reaction-field (SCRF) method (*45*). IEFPCM was adopted as it is a non-expensive computation and was successful in dealing with the electron transfer systems (*46*−*48*). Initially, one explicit water molecule in bulk water was included in the optimization of PBSA to evaluate the effect of hydrogen bonding. The computed E_{S1}, E_{T1}, VIE, and VEA values (Table S1) showed no significant difference from those obtained without the explicit water molecule (Table 2). Thus, the hydrogen bonding formed between water and PBSA was not considered in the subsequent computations. Nevertheless, the insignificance of hydrogen bonding cannot be a generalized rule, which should not be extrapolated to other organic pollutants. Details on the computations are presented in the SI.

Photodegradation Experiments. Experiments were performed employing a merry-go-round photoreactor (Xujiang, China) with quartz tubes containing PBSA solutions. The light source was a water-refrigerated 500-W high-pressure mercury lamp equipped with 365-nm filters to mimic the UVA and UVB portions of sunlight. The emission spectrum is shown in Figure S4. Dark controls were included for every batch of the treatments, and no loss of PBSA was observed in the dark.

The effects of O_2 were examined in aerated or N_2 saturated solutions. The roles of ROS were examined using D_2O, hematoporphyrin dihydrochloride (HPDHC), and *p*-benzoquinone (BQ) in aerated solutions. D_2O was employed to prolong the lifetime of $^1O_2$ (*49*), and therefore to facilitate the oxidation involving $^1O_2$. HPDHC was employed to generate $^1O_2$ and $O_2^{-}\cdot$ (*50*). BQ was used to scavenge $O_2^{-}\cdot$ (*50, 51*). The pH-dependence of photolysis kinetics was examined in pure water adjusted with H_2SO_4 and NaOH solutions. Photolysis quantum yields were determined at pH = 1, 7, and 14, with *p*-nitroanisole/pyridine (PNA/pyr) employed as a chemical actinometer (*52*).

The influence of SRFA, X^-, and HCO_3^-/CO_3^{2-} on photodegradation kinetics was investigated in phosphate buffer solutions (pH = 8). The observed photolysis rate constant (k_{obs}) in the presence of SRFA was corrected by the light screening factors (S_λ) (*19*) to obtain the direct/self-sensitized photolysis rate constant (k_{d+s}) and the indirect photolysis rate constant (k_{ind}). Detailed descriptions are presented in the SI.

Analytical Methods. Details on the analytical methods are presented in the SI.

Results and Discussion

Photodegradation Mechanism of PBSA Indicated by DFT. The computed values for E_{S1}, E_{T1}, VEA, and VIE are listed in Table 2. For PBSA0/PBSA-H/PBSA-2H, $E_{S1} - E_{T1} < E_\Sigma$ (1.627 eV (*36*)), and $E_{T1} > E_\Sigma$. It may thus be concluded that $PBSA^*_{T1}$ can photogenerate the $^1\Sigma_g^+$ state of $^1O_2$. For PBSA0/PBSA-H, $E_{S1} - E_{T1} > E_\Delta$ (0.974 eV (*36*)), and for PBSA0/PBSA-H/PBSA-2H, $E_{T1} > E_\Delta$, implying that the photogeneration of the $^1\Delta_g$

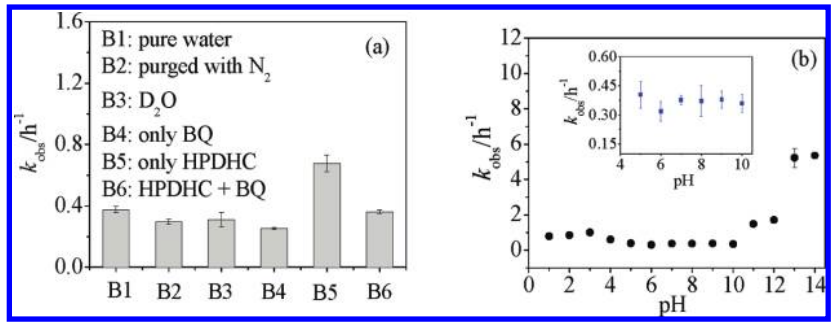

FIGURE 1. Photolysis rate constant (k_{obs}) of PBSA under different conditions: (a) without O_2, or in the presence of D_2O, HPDHC and BQ, pH = 7; (b) pH ranges 1−14. The initial concentration of PBSA is 1 mg L^{-1}. The error bars indicate 95% confidence intervals (n = 3).

state of $^1O_2$ is possible. The results indicate that both PBSA$^*_{S1}$ and PBSA$^*_{T1}$ can photogenerate $^1O_2$.

At the B3LYP/6-311++G(d,p) level, AEA($^3O_2$) = −3.684 eV. The computed values for ΔG of $O_2^{-}\cdot$ generation are listed in Table S2. For the electron transfer from PBSA0*/PBSA-H*/PBSA-2H* to $^3O_2$, $\Delta G_1 < 0$, indicating $O_2^{-}\cdot$ could be generated through direct electron transfer. For the autoionization between PBSA$_{S0}$ and PBSA$^*_{S1/T1}$, ΔG_2 and $\Delta G_3 > 0$, implying nonspontaneity of the reaction. However, PBSA$^{-}\cdot$ could be generated from the autoionization between two PBSA$^*_{S1/T1}$ molecules, since $\Delta G_4 < 0$. Moreover, $\Delta G_5 < 0$ for the electron transfer from PBSA$^{-}\cdot$ to $^3O_2$, indicating spontaneity of $O_2^{-}\cdot$ generation via PBSA$^*_{S1/T1}$ autoionization.

From these results, the photosensitizing pathways of PBSA are proposed as presented in Figure S5. Inbaraj et al. (*12*) detected $^1O_2$ and $O_2^{-}\cdot$ in irradiated PBSA solutions and the current study clarified the generating pathways of the ROS. $^1O_2$ and $O_2^{-}\cdot$ can induce subsequent oxidations, implying that the photodegradation of PBSA may involve the mechanism of self-sensitized photooxidation. The subsequent experimental results further confirm the roles of these ROS.

According to the ΔG_1 and ΔG_5 values (Table S2), all three protonation states can transfer an electron to $^3O_2$ and generate $O_2^{-}\cdot$. According to the VIE values of PBSA$^*_{S1/T1}$, the EDA of PBSA-2H$^*_{S1/T1}$ is the strongest, followed by PBSA-H and PBSA0. As the PBSA protonation states are pH-dependent (*12, 13*), the $O_2^{-}\cdot$ formation rate differs at different pH. Thus, it can be inferred that if $O_2^{-}\cdot$ was involved in the photooxidation of PBSA, the photolysis rate should be pH-dependent.

Effects of Water Constituents on PBSA Photodegradation Implied by DFT. The E_{T1} values of the DOM analogs (ADOM) are listed in Table 2. The values are close to those determined for the significant fractions of DOM (2.591 eV (*53*)), but higher than the mean values (1.762−1.866 eV) of the whole DOM (*54*). Obviously, the E_{T1} values for ADOM are lower than E_{T1}(PBSA). Therefore, PBSA cannot be sensitized by ADOM$^*_{T1}$ via energy transfer. Boreen et al. (*20*) and Canonica et al (*21*) also found that DOM or DOM triplet state models could not sensitize photodegradation of sulfa drugs and phenylurea herbicides by energy transfer. On the contrary, ADOM$_{S0}$ can accept the energy transfer from PBSA$^*_{T1}$, as E_{T1}(PBSA) > E_{T1}(ADOM). Therefore, in the view of the energy transfer pathway, the DOM analog inhibits the photodegradation by scavenging PBSA$^*_{T1}$.

According to the computed VEA$_{S0}$ values (Table 2), EAA of ADOM decreases in the order: LHA > CSHA > ARHA > SRFA. The order is consistent with the observation of Aeschbacher et al. (*55*) that the EAA of terrestrial HA is the strongest, followed by aquatic HA and FA. ΔG_6 values for the electron transfer from PBSA$_{S0}$ to ADOM$^*_{T1}$ are listed in Table S3. The results indicate that electron transfer from PBSA-2H$_{S0}$ to CSHA$^*_{T1}$/LHA$^*_{T1}$ is spontaneous to form radical ion pairs. It has been established that the photosensitization of amines by DOM$^*_{T1}$ proceeds through initial electron transfer from the N-electron of the amines to DOM$^*_{T1}$ and is followed by α-H transfer and radical formation reactions (*14, 56, 57*). Without α-H, the initial radical pairs cannot form stable separated radicals and will be quenched (*14, 56*). As PBSA has no α-H, the initial electron transfer from PBSA-2H$_{S0}$ to CSHA$^*_{T1}$/LHA$^*_{T1}$ would be followed by charge destruction and radical quenching. Electron transfer from ADOM$^*_{T1}$ to PBSA$_{S0}$ was also evaluated by ΔG_7 to be nonspontaneous. Therefore, PBSA$_{S0}$ cannot be photosensitized by ADOM$^*_{T1}$. It needs to be pointed out that computational results cannot fully represent bulk DOM from different origins as ADOM employed for the computation are structurally different from bulk DOM.

The computed $\Delta G_8 - \Delta G_{10}$ values for N_3^- are listed in Table S4, which are employed to validate the computational method for evaluating electron transfer between PBSA* and anions. The verification details provided in the SI confirmed that the computational method could be applied to evaluate the electron transfer between PBSA* and anions. The computed values of VIE and $\Delta G_8 - \Delta G_{10}$ for the anions are listed in Table 2 and Table S4, respectively. ΔG_8 for PBSA$^*_{S1}$ indicates that electron transfer from I^- to PBSA0$_{S1}$/PBSA-H$_{S1}$ and from CO_3^{2-} to PBSA$^*_{S1}$ is spontaneous. The value of ΔG_9 for PBSA$^*_{T1}$ implies that the electron transfer from CO_3^{2-} to PBSA0$^*_{T1}$/PBSA-H$^*_{T1}$ is spontaneous, whereas the transfer from the other anions is nonspontaneous. The value of ΔG_{10} for PBSA$^{+}\cdot$ suggests that electron transfer from Br^- to PBSA0$^{+}\cdot$, from I^- to PBSA0$^{+}\cdot$/PBSA-H$^{+}\cdot$, and from CO_3^{2-} to PBSA$^{+}\cdot$ is spontaneous. The electron transfer from the anions to PBSA$^*_{S1/T1}$ generates charge-transfer complexes. The separation of the radical ions is determined by the trapping of the primary charge-transfer complex by a second inorganic ion (*58*). The electron transfer from the anions to PBSA$^{+}\cdot$ induces regeneration of PBSA$_{S0}$ and inhibits the photodegradation. The photosensitization between PBSA and the main water constituents is illustrated in Figure S5.

Experimental Verification of Self-Sensitized Photolysis. The photolysis of PBSA in pure water followed pseudo-first-order kinetics ($r > 0.99$, $p < 0.05$, Figure S6). k_{obs} was observed to be dependent on c_0 (Figure S7) and decreased when O_2 was purged by N_2 (Figure 1a). The results indicate that PBSA undergoes both direct and self-sensitized photolysis, which is consistent with the computational predictions.

No evident change in k_{obs} was observed in D_2O, indicating that $^1O_2$ was not involved in the photolysis. In the presence of HPDHC, k_{obs} increased (Figure 1a). In the presence of BQ, k_{obs} slightly decreased. However, in the presence of both HPDHC and BQ, k_{obs} was similar to that in pure water (Figure 1a). As HPDHC can photogenerate $^1O_2$ and $O_2^{-}\cdot$, and BQ is capable of quenching $O_2^{-}\cdot$, $O_2^{-}\cdot$ was inferred to be involved in the photodegradation. The DFT results indicate that PBSA itself can photogenerate $O_2^{-}\cdot$. Thus, PBSA could undergo $O_2^{-}\cdot$ induced self-sensitized photodegradation. Serpone et al. (*25*) also observed that the filtering efficiency decay of PBSA in water was dependent on dissolved O_2, and they

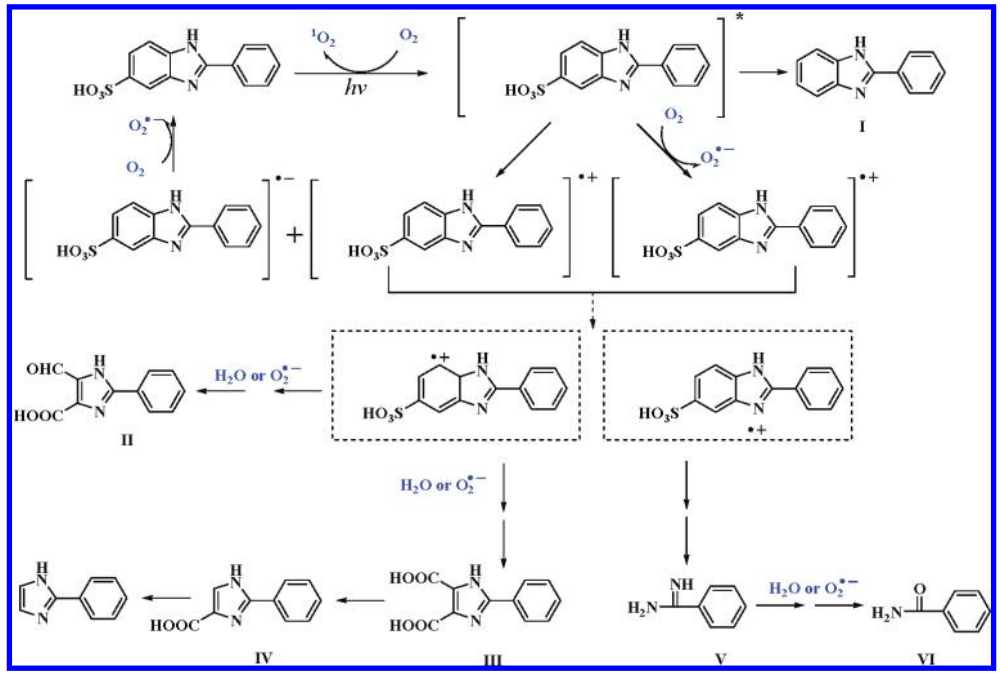

FIGURE 2. Photodegradation products and pathways of PBSA in pure water.

proposed the involvement of ROS. The present study further clarified the photogeneration pathway and role of $O_2^{-}\cdot$ in the photodegradation of PBSA.

Experimental Verification of the pH Dependence. As shown in the insert of Figure 1b, k_{obs} varies insignificantly within pH = 5−10, but increases at pH < 5 or >10 (Figure 1b). The results are consistent with results reported by Inbaraj et al. (*12*) and Zhang et al. (*59*) who determined the photolysis rate of PBSA at pH = 7 and 12, and found that PBSA photodegraded faster in basic solutions than in neutral solutions. The light absorption ($\Sigma L_\lambda \varepsilon_\lambda$) and photolysis quantum yields at pH = 1, 7, and 14 are listed in Table S6. The experiment confirmed the DFT predictions, i.e., the PBSA photolytic rate was pH dependent.

According to the distribution of the protonation states of PBSA (Figure S9), PBSA0, PBSA-H, and PBSA-2H are dominant species in solutions at pH = 1, 7, and 14, respectively. Based on the k_{obs} values (Figure 1b), the photolability of PBSA follows the order PBSA-2H > PBSA0 > PBSA-H. Their $\Sigma L_\lambda \varepsilon_\lambda$ values follow the order PBSA0 > PBSA-2H > PBSA-H. Therefore, light absorption is not the main factor differentiating the photolability. According to the DFT results, EDA of PBSA-2H was the least unfavorable, and the formation of $O_2^{-}\cdot$ by PBSA-2H photosensitization was the most favorable among the three PBSA species. Thus, the fastest photodegradation of PBSA-2H is most probably due to the $O_2^{-}\cdot$ induced self-sensitized photodegradation pathway. The DFT computation also indicates that the EDA of PBSA-H is stronger than the EDA of PBSA0. However, k_{obs} of PBSA0 was slightly higher than k_{obs} of PBSA-H, which could be due to the larger $\Sigma L_\lambda \varepsilon_\lambda$ value and the faster dismutation of $O_2^{-}\cdot$ in acidic solutions to form the stronger oxidant ·OH (*50*).

Photodegradation Products and Pathways. Based on the MS/MS spectra, six photodegradation products in pure water were identified and possible structures were proposed (Figure S10). Compound I (M_w 194) was identified as a desulfonated product. Compounds II (M_w 216), III (M_w 232), and IV (M_w 188) were formed from the cleavage of the benzene ring adjacent to the imidazole ring. Compounds V (M_w 120) and VI (M_w 121) were produced from opening of the imidazole ring. Zhang et al. (*59*) also observed products generated from the cleavage of the imidazole ring in irradiated basic solutions of PBSA.

The products were formed from both direct photolysis and self-sensitized photodegradation (Figure 2). PBSA* can lose one electron to form $PBSA^{+}\cdot$. According to the DFT results, $PBSA^{+}\cdot$ can be generated in two ways: autoionization and electron transfer from PBSA* to $^3O_2$. Bond cleavage of $PBSA^{+}\cdot$ may produce transition products, and the transition products react with $\cdot O_2^{-}$ or H_2O, leading to the final products.

Water Constituent Effects. The values of k_{obs}, k_{d+s}, and k_{ind} determined in the presence of SRFA are listed in Table S7. k_{d+s} decreased with the increase of SRFA, proving that the direct/self-sensitized photolysis of PBSA was inhibited by SRFA. k_{ind} increased with the increase of SRFA, implying that SRFA could sensitize the indirect photolysis of PBSA. SRFA competes for light absorption and $^3O_2$ with $PBSA_{S0}$, and SRFA scavenges $PBSA^*_{T1}$ as predicted by DFT. Thus, the DFT predictions are confirmed by the experiment. According to the DFT results (Table S3), PBSA cannot be sensitized by $SRFA^*_{T1}$. As it has been clarified that PBSA cannot react with $^1O_2$ (Figure 1a), and SRFA can photogenerate $^1O_2$ and ·OH (*14*), the indirect photolysis of PBSA is most probably induced by ·OH.

The experimental results indicated that the photodegradation of PBSA was inhibited by X^- significantly and HCO_3^-/CO_3^{2-} slightly (Figure S11 and Table S8). At pH = 8, PBSA exists mainly as PBSA-H. As the computational results indicate that the electron transfer from Cl^-/Br^- to $PBSA^*_{S1/T1}/PBSA^{+}\cdot$ is nonspontaneous, the inhibiting effects of Cl^-/Br^- on the photodegradation could be attributed to physical quenching. According to the DFT results, the electron transfer from I^- to $PBSA^*_{S1/T1}/PBSA^{+}\cdot$ is spontaneous. Therefore, I^- inhibited the photodegradation by transferring electrons to $PBSA^*_{S1/T1}/PBSA^{+}\cdot$, in addition to a possible physical quenching mechanism. At pH = 8, HCO_3^- is the dominant species (91%) of HCO_3^-/CO_3^{2-} (*60*), and the DFT predicts that the electron transfer from HCO_3^- to $PBSA_{S1/T1}/PBSA^{+}\cdot$ is nonspontaneous. Therefore, physical quenching of $PBSA^*_{S1/T1}/PBSA^{+}\cdot$ by HCO_3^-/CO_3^{2-} is the most probable mechanism for the marginal inhibiting effects.

This study indicates that DFT provides valuable information on the photodegradation pathways that is verified by the experiment or supports the mechanism interpretation. Thus, DFT can be an important tool for assessing environmental photochemical behavior of pollutants.

Acknowledgments

Prof. Qingyu Zhang is greatly acknowledged for the measurement of the lamp irradiance. Prof. W. Peijnenburg is greatly acknowledged for valuable suggestions to polish the paper. The study was supported by the National Basic Research Program (2006CB403302), National Natural Science Foundation (20777010), and the Program for Changjiang Scholars and Innovative Research Team in University (IRT0813) of P. R. China.

Supporting Information Available

Detailed description of the computational and experimental methods, distribution of the protonation states of PBSA, molecular structures of the DOM analogs, energy/electron transfer reactions suggested by DFT, lamp emission spectrum, photolytic kinetics curves, PBSA absorption spectra, MS/MS spectra, computational results for PBSA with one explicit water molecule, computed ΔG values, computational results for PBSA at the B3LYP/LANL2DZ level, experimentally determined photolysis quantum yields, and photolysis rate constant values in the presence of water constituents. This material is available free of charge via the Internet at http://pubs.acs.org.

Literature Cited

(1) Schwarzenbach, R. P.; Escher, B. I.; Fenner, K.; Hofstetter, T. B.; Johnson, C. A.; Von Gunten, U.; Wehrli, B. The challenge of micropollutants in aquatic systems. *Science* **2006**, *313* (5790), 1072–1077.

(2) Diaz-Cruz, M. S.; Llorca, M.; Barcelo, D. Organic UV filters and their photodegradates, metabolites and disinfection by-products in the aquatic environment. *Trac-Trends Anal. Chem.* **2008**, *27* (10), 873–887.

(3) Rodil, R.; Quintana, J. B.; Lopez-Mahia, P.; Muniategui-Lorenzo, S.; Prada-Rodriguez, D. Multiclass determination of sunscreen chemicals in water samples by liquid chromatography−tandem mass spectrometry. *Anal. Chem.* **2008**, *80* (4), 1307–1315.

(4) Balmer, M. E.; Buser, H. R.; Muller, M. D.; Poiger, T. Occurrence of some organic UV filters in wastewater, in surface waters, and in fish from Swiss lakes. *Environ. Sci. Technol.* **2005**, *39* (4), 953–962.

(5) Buser, H. R.; Balmer, M. E.; Schmid, P.; Kohler, M. Occurrence of UV filters 4-methylbenzylidene camphor and octocrylene in fish from various Swiss rivers with inputs from wastewater treatment plants. *Environ. Sci. Technol.* **2006**, *40* (5), 1427–1431.

(6) Morohoshi, K.; Yamamoto, H.; Kamata, R.; Shiraishi, F.; Koda, T.; Morita, M. Estrogenic activity of 37 components of commercial sunscreen lotions evaluated by in vitro assays. *Toxicol. in Vitro* **2005**, *19* (4), 457–469.

(7) Kunz, P. Y.; Fent, K. Estrogenic activity of UV filter mixtures. *Toxicol. Appl. Pharmacol.* **2006**, *217* (1), 86–99.

(8) Rodil, R.; Moeder, M.; Altenburger, R.; Schmitt-Jansen, M. Photostability and phytotoxicity of selected sunscreen agents and their degradation mixtures in water. *Anal. Bioanal. Chem.* **2009**, *395* (5), 1513–1524.

(9) Hayashi, T.; Okamoto, Y.; Ueda, K.; Kojima, N. Formation of estrogenic products from benzophenone after exposure to sunlight. *Toxicol. Lett.* **2006**, *167* (1), 1–7.

(10) Allen, J. M.; Gossett, C. J.; Allen, S. K. Photochemical formation of singlet molecular oxygen ($^1O_2$) in illuminated aqueous solutions of *p*-aminobenzoic acid (PABA). *J. Photochem. Photobiol., B* **1996**, *32* (1−2), 33–37.

(11) Allen, J. M.; Gossett, C. J.; Allen, S. K. Photochemical formation of singlet molecular oxygen in illuminated aqueous solutions of several commercially available sunscreen active ingredients. *Chem. Res. Toxicol.* **1996**, *9* (3), 605–609.

(12) Inbaraj, J. J.; Bilski, P.; Chignell, C. F. Photophysical and photochemical studies of 2-phenylbenzimidazole and UVB sunscreen 2-phenylbenzimidazole-5-sulfonic acid. *Photochem. Photobiol.* **2002**, *75* (2), 107–116.

(13) Stevenson, C.; Davies, R. J. H. Photosensitization of guanine-specific DNA damage by 2-phenylbenzimidazole and the sunscreen agent 2-phenylbenzimidazole-5-sulfonic acid. *Chem. Res. Toxicol.* **1999**, *12* (1), 38–45.

(14) Chen, Y.; Hu, C.; Hu, X. X.; Qu, J. H. Indirect photodegradation of amine drugs in aqueous solution under simulated sunlight. *Environ. Sci. Technol.* **2009**, *43* (8), 2760–2765.

(15) Ge, L. K.; Chen, J. W.; Lin, J.; Cai, X. Y. Light-source-dependent effects of main water constituents on photodegradation of phenicol antibiotics: mechanism and kinetics. *Environ. Sci. Technol.* **2009**, *43* (9), 3101–3107.

(16) Ge, L. K.; Chen, J. W.; Wei, X. X.; Zhang, S. Y.; Qiao, X. L.; Cai, X. Y.; Xie, Q. Aquatic photochemistry of fluoroquinolone antibiotics: kinetics, pathways, and multivariate effects of main water constituents. *Environ. Sci. Technol.* **2010**, *44* (7), 2400–2405.

(17) Werner, J. J.; Arnold, W. A.; McNeill, K. Water hardness as a photochemical parameter: Tetracycline photolysis as a function of calcium concentration, magnesium concentration, and pH. *Environ. Sci. Technol.* **2006**, *40* (23), 7236–7241.

(18) Edhlund, B. L.; Arnold, W. A.; McNeill, K. Aquatic photochemistry of nitrofuran antibiotics. *Environ. Sci. Technol.* **2006**, *40* (17), 5422–5427.

(19) Walse, S. S.; Morgan, S. L.; Kong, L.; Ferry, J. L. Role of dissolved organic matter, nitrate, and bicarbonate in the photolysis of aqueous fipronil. *Environ. Sci. Technol.* **2004**, *38* (14), 3908–3915.

(20) Boreen, A. L.; Arnold, W. A.; McNeill, K. Triplet-sensitized photodegradation of sulfa drugs containing six-membered heterocyclic groups: Identification of an SO_2 extrusion photoproduct. *Environ. Sci. Technol.* **2005**, *39* (10), 3630–3638.

(21) Canonica, S.; Hellrung, B.; Müller, P.; Wirz, J. Aqueous Oxidation of Phenylurea Herbicides by Triplet Aromatic Ketones. *Environ. Sci. Technol.* **2006**, *40* (21), 6636–6641.

(22) Sakkas, V. A.; Giokas, D. L.; Lambropoulou, D. A.; Albanis, T. A. Aqueous photolysis of the sunscreen agent octyl-dimethyl-*p*-aminobenzoic acid - Formation of disinfection byproducts in chlorinated swimming pool water. *J. Chromatogr., A* **2003**, *1016* (2), 211–222.

(23) Giokas, D. L.; Vlessidis, A. G. Application of a novel chemometric approach to the determination of aqueous photolysis rates of organic compounds in natural waters. *Talanta* **2007**, *71* (1), 288–295.

(24) Klein, J.; Tse, M. L.; MacManus-Spencer, L. A. Photochemical degradation of ultraviolet filter chemicals in surface waters. In *Abstracts of Papers, 237th ACS National Meeting, ENVR-157, Salt Lake City, UT*; American Chemical Society, Division of Environmental Chemistry, March 22−26, 2009.

(25) Serpone, N.; Salinaro, A.; Emeline, A. V.; Horikoshi, S.; Hidaka, H.; Zhao, J. C. An *in vitro* systematic spectroscopic examination of the photostabilities of a random set of commercial sunscreen lotions and their chemical UVB/UVA active agents. *Photochem. Photobiol. Sci.* **2002**, *1* (12), 970–981.

(26) Allen, J. M.; Engenolf, S.; Allen, S. K. Rapid reaction of singlet molecular oxygen ($^1O_2$) with *p*-aminobenzoic acid (PABA) in aqueous solution. *Biochem. Biophys. Res. Commun.* **1995**, *212* (3), 1145–1151.

(27) Shaw, A. A.; Wainschel, L. A.; Shetla, M. D. The photochemistry of *p*-aminobenzoic acid. *Photochem. Photobiol.* **1992**, *55* (5), 647–656.

(28) Reeser, D. I.; Jammoul, A.; Clifford, D.; Brigante, M.; D'Anna, B.; George, C.; Donaldson, D. J. Photoenhanced reaction of ozone with chlorophyll at the seawater surface. *J. Phys. Chem. C* **2009**, *113* (6), 2071–2077.

(29) Jammoul, A.; Dumas, S.; D'Anna, B.; George, C. Photoinduced oxidation of sea salt halides by aromatic ketones: a source of halogenated radicals. *Atmos. Chem. Phys.* **2009**, *9* (13), 4229–4237.

(30) Canonica, S.; Kohn, T.; Mac, M.; Real, F. J.; Wirz, J.; Von Gunten, U. Photosensitizer method to determine rate constants for the reaction of carbonate radical with organic compounds. *Environ. Sci. Technol.* **2005**, *39* (23), 9182–9188.

(31) Kuzmin, V. A.; Chibisov, A. K.; Karyakin, A. V. Decay kinetics of the triplet and anthrasemiquinone radicals in aqueous organic media. *Int. J. Chem. Kinet.* **1972**, *4* (6), 639–644.

(32) Chiron, S.; Minero, C.; Vione, D. Photodegradation processes of the antiepileptic drug carbamazepine, relevant to estuarine waters. *Environ. Sci. Technol.* **2006**, *40* (19), 5977–5983.

(33) Liu, H.; Zhao, H. M.; Quan, X.; Zhang, Y. B.; Chen, S. Formation of chlorinated intermediate from bisphenol A in surface saline water under simulated solar light irradiation. *Environ. Sci. Technol.* **2009**, *43* (20), 7712–7717.

(34) Ji, H. F.; Shen, L. Triplet excited state characters and photosensitization mechanisms of α-terthienyl: a theoretical study. *J. Photochem. Photobiol., B* **2009**, *94* (1), 51–53.

(35) Wang, Y.; Chen, J. W.; Ge, L. K.; Wang, D. G.; Cai, X. Y.; Huang, L. P.; Hao, C. Experimental and theoretical studies on the

photoinduced acute toxicity of a series of anthraquinone derivatives towards the water flea (*Daphnia magna*). *Dyes Pigments* **2009**, *83* (3), 276–280.
(36) Schweitzer, C.; Schmidt, R. Physical mechanisms of generation and deactivation of singlet oxygen. *Chem. Rev.* **2003**, *103* (5), 1685–1757.
(37) Kavarnos, G. J.; Turro, N. J. Photosensitization by reversible electron-transfer - theories, experimental-evidence, and examples. *Chem. Rev.* **1986**, *86* (2), 401–449.
(38) Niederer, C.; Goss, K. U. Quantum chemical modeling of humic acid/air equilibrium partitioning of organic vapors. *Environ. Sci. Technol.* **2007**, *41* (10), 3646–3652.
(39) Diallo, M. S.; Simpson, A.; Gassman, P.; Faulon, J. L.; Johnson, J. H.; Goddard, W. A.; Hatcher, P. G. 3-D structural modeling of humic acids through experimental characterization, computer assisted structure elucidation and atomistic simulations. 1. Chelsea soil humic acid. *Environ. Sci. Technol.* **2003**, *37* (9), 1783–1793.
(40) Wilson, M. A.; Vassallo, A. M.; Perdue, E. M.; Reuter, J. H. Compositional and solid-state nuclear-magnetic-resonance study of humic and fulvic-acid fractions of soil organic-matter. *Anal. Chem.* **1987**, *59* (4), 551–558.
(41) Leenheer, J. A.; McKnight, D. M.; Thurman, E. M.; MacCarthy, P. Structural components and proposed structural models of fulvic acid from the Suwannee River. *U.S. Geol. Surv. Water-Supply Pap.* **1995**, 195–211.
(42) Frisch, M. J.; et al. *Gaussian 09 Revision A.02.*; Gaussian Inc.: Wallingford, CT, 2009; detailed descriptions are presented in the SI.
(43) Silva-Junior, M. R.; Schreiber, M.; Sauer, S. P. A.; Thiel, W. Benchmarks for electronically excited states: Time-dependent density functional theory and density functional theory based multireference configuration interaction. *J. Chem. Phys.* **2008**, *129* (10), 104103.
(44) Jacquemin, D.; Perpète, E. A.; Ciofini, I.; Adamo, C. Assessment of functionals for TD-DFT calculations of singlet-triplet transitions. *J. Chem. Theory Comput.* **2010**, *6* (5), 1532–1537.
(45) Tomasi, J.; Mennucci, B.; Cammi, R. Quantum mechanical continuum solvation models. *Chem. Rev.* **2005**, *105* (8), 2999–3093.
(46) Blotevogel, J.; Borch, T.; Desyaterik, Y.; Mayeno, A. N.; Sale, T. C. Quantum chemical prediction of redox reactivity and degradation pathways for aqueous phase contaminants: An example with HMPA. *Environ. Sci. Technol.* **2010**, *44* (15), 5868–5874.
(47) Kaledin, A. L.; Huang, Z. Q.; Yin, Q. S.; Dunphy, E. L.; Constable, E. C.; Housecroft, C. E.; Geletii, Y. V.; Lian, T. Q.; Hill, C. L.; Musaev, D. G. Insights into photoinduced electron transfer between $[Ru(mptpy)_2]^{4+}$ (mptpy = 4′(4-methylpyridinio)-2,2′:6′,2″-terpyridine) and $[S_2O_8]^{2-}$: Computational and experimental studies. *J. Phys. Chem. A* **2010**, *114* (21), 6284–6297.
(48) Namazian, M.; Almodarresieh, H. A.; Noorbala, M. R.; Zare, H. R. DFT calculation of electrode potentials for substituted quinones in aqueous solution. *Chem. Phys. Lett.* **2004**, *396* (4−6), 424–428.
(49) Wilkinson, F.; Helman, W. P.; Ross, A. B. Rate constants for the decay and reactions of the lowest electronically excited singlet-state of molecular-oxygen in solution - an expanded and revised compilation. *J. Phys. Chem. Ref. Data* **1995**, *24* (2), 663–1021.
(50) Herath, A. C.; Rajapakse, R. M. G.; Wicramasinghe, A.; Karunaratne, V. Photodegradation of triphenylamino methane (magenta) by photosensitizer in oxygenated solutions. *Environ. Sci. Technol.* **2009**, *43* (1), 176–180.
(51) Chen, Y.; Hu, C.; Qu, J. H.; Yang, M. Photodegradation of tetracycline and formation of reactive oxygen species in aqueous tetracycline solution under simulated sunlight irradiation. *J. Photochem. Photobiol., A* **2008**, *197* (1), 81–87.
(52) Dulln, D.; Mill., T. Development and evaluation of sunlight actinometers. *Environ. Sci. Technol.* **1982**, *16* (11), 815–820.
(53) Zepp, R. G.; Schlotzhauer, P. F.; Sink, R. M. Photosensitized transformations involving electronic energy transfer in natural waters: Role of humic substances. *Environ. Sci. Technol.* **1985**, *19* (1), 74–81.
(54) Bruccoleri, A.; Pant, B. C.; Sharma, D. K.; Langford, C. H. Evaluation of primary photoproduct quantum yields in fulvic acid. *Environ. Sci. Technol.* **1993**, *27* (5), 889–894.
(55) Aeschbacher, M.; Sander, M.; Schwarzenbach, R. P. Novel electrochemical approach to assess the redox properties of humic substances. *Environ. Sci. Technol.* **2010**, *44* (1), 87–93.
(56) Cohen, S. G.; Davis, G. A.; Clark, W. D. K. Photoreduction of π, π^* triplets by amines, 2-naphthaldehyde, and 2-acetonaphthone. *J. Am. Chem. Soc.* **1972**, *94* (3), 869–874.
(57) Cohen, S. G.; Parola, A.; Parsons, G. H. Photoreduction by amines. *Chem. Rev.* **1973**, *73* (2), 141–161.
(58) Mac, M.; Wirz, J.; Najbar, J. Transient radicals formed by electron-transfer between inorganic-ions and excited aromatic-molecules in polar-solvents. *Helv. Chim. Acta* **1993**, *76* (3), 1319–1331.
(59) Zhang, W.; Wilson, C. R.; Danielson, N. D. Indirect fluorescent determination of selected nitro-aromatic and pharmaceutical compounds via UV-photolysis of 2-phenylbenzimidazole-5-sulfonate. *Talanta* **2008**, *74* (5), 1400–1407.
(60) Bouillon, R. C.; Miller, W. L. Photodegradation of dimethyl sulfide (DMS) in natural waters: Laboratory assessment of the nitrate-photolysis-induced DMS oxidation. *Environ. Sci. Technol.* **2005**, *39* (24), 9471–9477.

ES101131H